JACS
JOURNAL OF THE AMERICAN CHEMICAL SOCIETY
Article
pubs.acs.org/JACS

Multiphonon Relaxation Slows Singlet Fission in Crystalline Hexacene

Erik Busby,[†,‡,∥] Timothy C. Berkelbach,[¶,∥] Bharat Kumar,[¶,∥] Alexey Chernikov,[§] Yu Zhong,[¶] Htay Hlaing,[§] X.-Y. Zhu,[¶] Tony F. Heinz,[§] Mark S. Hybertsen,[‡] Matthew Y. Sfeir,[‡] David R. Reichman,[¶] Colin Nuckolls,[¶] and Omer Yaffe*[,†,‡]

[†]Energy Frontier Research Center, [¶]Department of Chemistry, and [§]Departments of Physics and Electrical Engineering, Columbia University, New York, New York 10027, United States

[‡]Center for Functional Nanomaterials, Brookhaven National Laboratory, Upton, New York 11973-5000, United States

Supporting Information

ABSTRACT: Singlet fission, the conversion of a singlet excitation into two triplet excitations, is a viable route to improved solar-cell efficiency. Despite active efforts to understand the singlet fission mechanism, which would aid in the rational design of new materials, a comprehensive understanding of mechanistic principles is still lacking. Here, we present the first study of singlet fission in crystalline hexacene which, together with tetracene and pentacene, enables the elucidation of mechanistic trends. We characterize the static and transient optical absorption and combine our findings with a theoretical analysis of the relevant electronic couplings and rates. We find a singlet fission time scale of 530 fs, which is orders of magnitude faster than tetracene (10−100 ps) but significantly slower than pentacene (80−110 fs). We interpret this increased time scale as a multiphonon relaxation effect originating from a large exothermicity and present a microscopic theory that quantitatively reproduces the rates in the acene family.

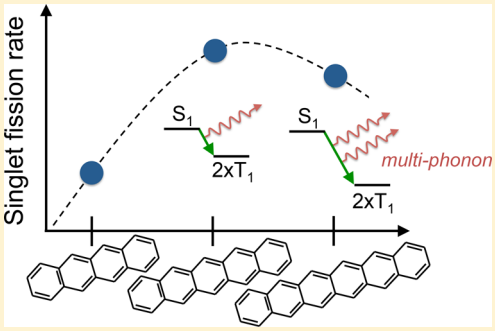

INTRODUCTION

Singlet fission (SF) is a spin-allowed energy conversion process that occurs in select organic molecules and aggregates where an excited singlet state converts into two triplet states on adjacent chromophores.[1,2] This form of carrier multiplication has recently attracted much attention as a means of improving upon the fundamental efficiency limitations of single junction photovoltaic cells.[3,4] While recent theoretical and experimental work has led to significant progress in the field, a complete and quantitative understanding of the variables that need to be optimized in order to exploit SF for photovoltaic applications is still far from complete.

The current understanding of SF suggests that the efficiency (i.e., singlet to triplet conversion ratio) and the rate of the SF process is governed mainly by two parameters: the energy difference between the excited singlet (S_1) and the multiexciton triplet pair (TT) states, $\Delta E_{SF} = 2E(T_1) - E(S_1)$ (where $2E(T_1) \approx E(TT)$), and the electronic coupling between these states, $V_{SF} = \langle S_1|H|TT\rangle$ (H is the electronic Hamiltonian). It is generally accepted that SF is most efficient in systems for which the process is exothermic ($\Delta E_{SF} < 0$) and the electronic coupling is large. The magnitude of the electronic coupling is strongly dependent on the intermolecular distance and orientation as well as the microscopic mechanism by which SF takes place. While there is an ongoing debate regarding the relative importance of different mechanisms, it is currently accepted that molecular systems with excited states that have strong charge-transfer (CT) character exhibit strong coupling between the low-lying excited singlet and triplet pair states.[2,5−10]

The elucidation of generic mechanistic features of SF has been hindered by the lack of materials which exhibit the phenomenon. The linear acenes, especially tetracene and pentacene, have received the most attention. These are perhaps the best understood SF systems, and they have proven to be some of the fastest and most efficient SF materials. With respect to energetics and considerations of electronic coupling, pentacene in particular satisfies the two key conditions for SF discussed above: the process is slightly exothermic ($-\Delta E_{SF} \approx$ 110−170 meV)[1,11] and the electronic coupling is reasonably large ($V_{SF} \approx$ 10−50 meV).[7,10,12] The strong electronic coupling has been linked to the large CT character of the S_1 state, which manifests as a large Davydov splitting (130 meV) seen in polarization-resolved absorption spectra.[9,13−15] These metrics have helped rationalize the extremely fast SF time scale in pentacene ($k_{SF}^{-1} \approx$ 80−110 fs).[11,16−18] Such a short time scale allows SF to out-compete other relaxation channels, leading to a high thermodynamic yield for the overall SF process. These properties of pentacene provide strong impetus for a systematic study of the larger acenes such as hexacene, for which the magnitudes of ΔE_{SF} and V_{SF} are expected to be even larger, in

Received: April 21, 2014
Published: July 1, 2014

   dx.doi.org/10.1021/ja503980c | J. Am. Chem. Soc. 2014, 136, 10654−10660

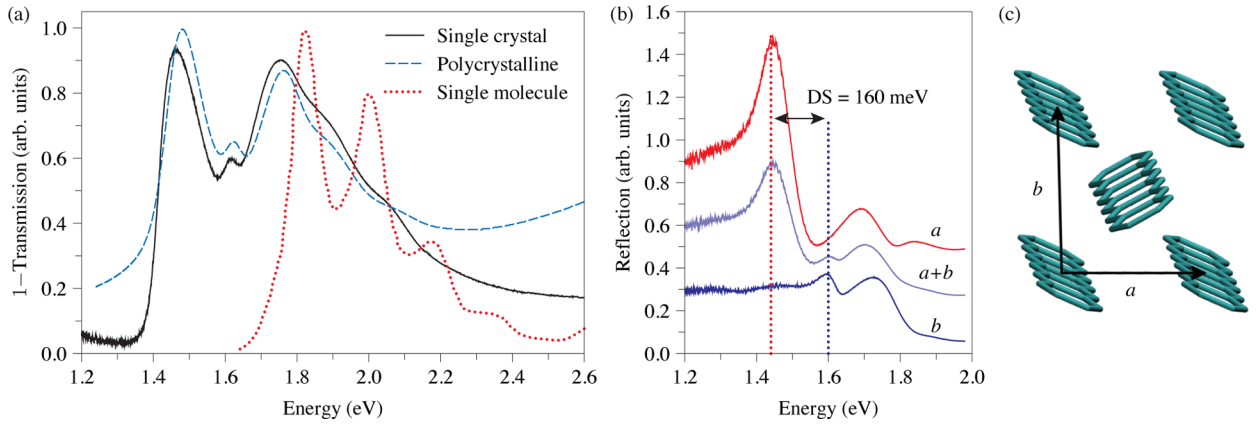

Figure 1. (a) Unpolarized transmission spectra of single crystal, polycrystalline, and solution-phase (single-molecule) hexacene (reproduced with permission from ref 23). (b) Reflection spectra of the single crystal with polarization parallel to the *a*, *a* + *b*, and *b* crystallographic directions, demonstrating the Davydov splitting of 160 meV. (c) Hexacene crystal structure and lattice vectors referenced in (b).

order to gain further insight into both fundamental and potentially practical aspects of SF.

Until recently, the photophysics of acenes larger than pentacene have been unobtainable, due to a lack of synthesis and preparation methods. In this work, we adopt a recently developed synthetic technique for producing high-quality, pure hexacene films and crystals[19] to experimentally study how aspects of the electronic structure influence SF rates in acene crystals. We report here the first experimental determination of the SF dynamics in hexacene which, together with tetracene and pentacene, allows for a systematic study of the influence of electronic properties on the SF rate.

A unique feature of hexacene is that the measured $E(S_1)$ is nearly three times the expected $E(T_1)$. Singlet fission in the regime where there exists both large exothermicity and large electronic coupling has not been previously explored. This allows for the possibility of two competing relaxation processes: SF into three triplets ($S_1 \rightarrow 3 \times T_1$) or SF into two triplets accompanied by the emission of high energy phonons ($S_1 \rightarrow 2 \times T_1$ + phonons). In order to understand the relative contributions of these two mechanisms, we characterize the static and dynamical optical absorption properties and combine our findings with a detailed theoretical analysis of the relevant electronic couplings and rates. Our analysis strongly suggests that the ($S_1 \rightarrow 2 \times T_1$ + phonons) SF mechanism predominates. We find a SF time scale of 530 fs, which is significantly faster than tetracene (10−100 ps)[20−22] but slower than pentacene (80−110 fs).[11,16−18]

RESULTS AND DISCUSSION

We begin by investigating the linear optical transitions of crystalline and polycrystalline hexacene, which will ultimately determine the thermodynamic driving forces for SF. Clearly, the energy difference between S_1 and the multiexciton TT states will depend sensitively on the molecular environment, given that molecular interactions, screening, and polarization effects can dramatically alter the electronic structure. In Figure 1a, we compare the room-temperature transmission spectra of single crystal hexacene, polycrystalline film, and the solution-phase single molecule (reproduced from ref 23). As expected, there is a strong solution-to-crystal redshift, yielding a decrease in $E(S_1)$ from 1.82 eV in solution to 1.48 eV in polycrystalline films and to 1.46 eV in the single crystal. While the molecular spectrum in solution exhibits the typical acene vibronic progression, the structure of the crystalline spectra is significantly different, and quite similar to pentacene crystals, suggesting that the higher lying peaks can be interpreted as various mixtures of Frenkel and CT exciton components.[9,13,15,24] We also note that $E(S_1)$ for pure hexacene is about 200 meV less than previously reported values for a substituted hexacene derivative,[25] which we interpret as the result of greater intermolecular coupling in the absence of steric effects from functional groups.

An experimental determination of ΔE_{SF} in the crystal would also require measuring $E(T_1)$. However, while the energy of the dipole-allowed singlet state for hexacene is readily determined with absorption measurements, the energy of the dipole-forbidden triplet state is much more difficult to measure precisely. In the smaller acenes (anthracene, tetracene, and pentacene), the crystal-phase triplet energy is rather uniformly 30−50 meV below that of the single-molecule triplet.[26−28] In hexacene, the single-molecule triplet energy is 540 meV,[23] suggesting that the crystal phase triplet energy is very close to 500 meV. Taken together, this suggests that the energy needed for the formation of two triplets is 1.0 eV and for three triplets is 1.5 eV. When compared to the singlet energies measured here, we find that SF to generate two triplets is strongly exothermic ($\Delta E_{SF}^{(2)} \approx -500$ meV) and SF to generate three triplets is slightly endothermic ($\Delta E_{SF}^{(3)} \approx 100$ meV). Nevertheless, it is important to note that we have neglected entropic contributions to the driving force as well as the possibility of a large triplet−triplet binding energy. As an example, SF in tetracene is slightly endothermic yet it is still efficient,[21,22] albeit dramatically slower than in the exothermic case of pentacene.

Next, we investigate the intermolecular electronic coupling in hexacene single crystals. Like the shorter members of the linear acene family, hexacene molecules arrange in a triclinic crystal structure with a herringbone motif (Figure 1c).[19] The presence of two translationally inequivalent molecules in the unit cell gives rise to a Davydov splitting (DS) of the exciton levels.[13] Importantly, a positive correlation between the magnitude of the DS and the degree of CT character in the low-lying excited states has recently been established in the family of acene crystals.[13] The magnitude of the Davydov splitting can frequently be inferred from the splitting of the first two peaks in the unpolarized absorption, and the data presented in Figure 1a suggest a DS of about 160 meV. To more conclusively identify these peaks as Davydov doublets, we have performed

dx.doi.org/10.1021/ja503980c | J. Am. Chem. Soc. 2014, 136, 10654−10660

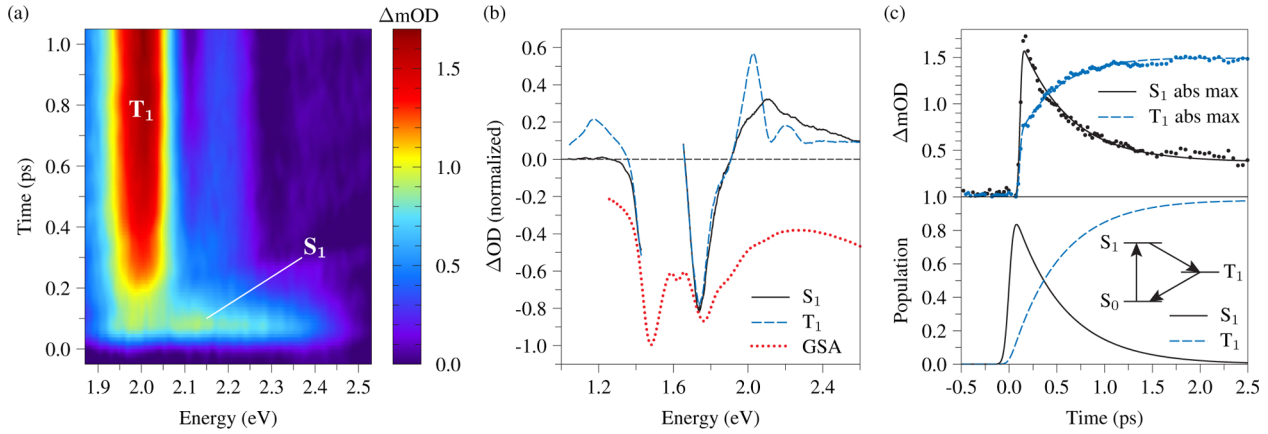

Figure 2. (a) Transient absorption signal as a function of time and probe energy (probe beam at 45°), highlighting the photoinduced absorption features of the singlet (S_1) and triplet (T_1). (b) Singlet and triplet photoinduced absorption spectra as extracted from global analysis. The strong negative signal at energies between 1.4 and 2.0 eV is associated with the ground-state bleach; inverted ground-state absorption (GSA) is shown for comparison. (c, top) Kinetic traces at S_1 and T_1 induced absorption maxima with exponential fits. (c, bottom) Singlet and triplet population kinetics extracted from global analysis, demonstrating the 530 fs singlet fission time scale. Inset depicts the three-state kinetic model used in global analysis to fit the TA data.

polarization-resolved reflection spectroscopy measurements. Figure 1b presents measured spectra on a high-quality single crystal of hexacene. The intensities of the first two peaks at 1.44 and 1.60 eV (slightly shifted in reflection when compared to transmission) strongly depend on the angle of the linearly polarized light. The effect of polarization angle is opposite for the two peaks: along the *a* crystallographic direction (see Figure 1c) the 1.44 eV peak reaches its maximum intensity while the 1.60 eV peak is eliminated and vice versa along the *b* crystallographic direction. This behavior confirms that the two peaks are a Davydov doublet with a DS of 160 meV. This value is indeed larger than the values reported for tetracene (∼80 meV)[22,29] and pentacene (∼130 meV),[18,30] suggesting that the degree of CT character in hexacene is very large. As discussed above, the electronic coupling V_{SF} which mediates conventional SF is therefore expected to be quite large.[2,7,9,15]

Such large CT character also has interesting implications for $V_{SF}^{(3)} = \langle S_1|H|TTT\rangle$, the electronic coupling which mediates the $(S_1 \rightarrow 3 \times T_1)$ process. Using a simple model consisting of six valence electrons on three neighboring molecules, one can consider Frenkel excitations, $|S_1S_0S_0\rangle$, and CT excitations, $|CAS_0\rangle$, where C and A denote cationic and anionic configurations on each molecule. One can show that $\langle S_1S_0S_0|H|TTT\rangle = 0$, i.e., pure Frenkel excitons do not couple (to lowest order) to a three-triplet multiexciton state (see Supporting Information). However, when the low-lying adiabatic states have CT character, i.e., $|S_1\rangle \sim \alpha|S_1S_0S_0\rangle + \beta|CAS_0\rangle$, then the CT component provides a first-order two-electron coupling and a second-order mediated coupling. This result is analogous to the usual case where Frenkel excitons couple to a two-triplet state via a two-electron integral, whereas CT excitons couple via a larger one-electron integral.[1,2,6] Therefore, we have the interesting result that strong CT character in S_1 increases the probability for SF to generate three triplets, just as has been concluded for SF to generate two triplets.[2,6,7,9] Nevertheless, although nonzero, these couplings can be inferred to be small due to the interplay of orbitals on three distinct molecules. This small electronic coupling combined with the likelihood of uphill, endothermic SF to generate three triplets strongly suggests that the process does not occur in crystalline hexacene, and we henceforth only consider the conventional mechanism to generate two triplets. The very fast time scale that we observe (vide infra) confirms this assumption, because it is roughly 2 orders of magnitude faster than tetracene, the fastest known endothermic system. However, it is interesting to note that for longer acenes (e.g., heptacene), the $(S_1 \rightarrow 3 \times T_1)$ pathway may become more competitive due to increased CT character and improved energetic alignment.

We now turn to the investigation of the excited-state dynamics to measure the rate of SF in hexacene. For that purpose, we use broadband femtosecond transient absorption (TA) spectroscopy on polycrystalline hexacene films (Figure 2). Hexacene films were excited at 1.49 eV, which corresponds to the lowest-energy electronic transition (Figure 1a). Pump-power dependence measurements were conducted to ensure that the excitation density was sufficiently low, so as to avoid singlet−singlet exciton annihilation and other nonlinear processes (see Supporting Information). Following excitation (17.6 $\mu J/cm^2$), two distinct induced absorption species are observed in Figure 2a: a short-lived, featureless absorption centered at 2.13 eV and long-lived feature showing two peaks at 2.0 and 2.2 eV (Figure 2b). The first feature is assigned as the singlet exciton (S_1), in qualitative agreement with other acene systems.[17,25] The second feature is assigned to the triplet exciton (T_1), in agreement with unsubstituted hexacene in solution[23] and substituted hexacene films.[25] This $T_1 \rightarrow T_n$ absorption band features a progression of peaks with 180 meV spacing that is characteristic of vibronic coupling to the ring-breathing mode in acene systems. We also note that the magnitude of the triplet induced absorption signal is dependent on the probe-substrate angle of incidence, due to the combined effects of molecular orientation nearly normal to the substrate surface and a triplet transition dipole that is oriented along the long axis of the molecule. As a result, the triplet TA signal is maximized with a large angle of incidence, which is in agreement with previous observations in pentacene.[27] All displayed TA data were acquired with the probe beam at 45° incidence; data acquired at normal incidence are presented in the Supporting Information.

To quantitatively validate the SF reaction scheme, obtain rate constants, and decompose the TA data into time-independent

dx.doi.org/10.1021/ja503980c | J. Am. Chem. Soc. 2014, 136, 10654−10660

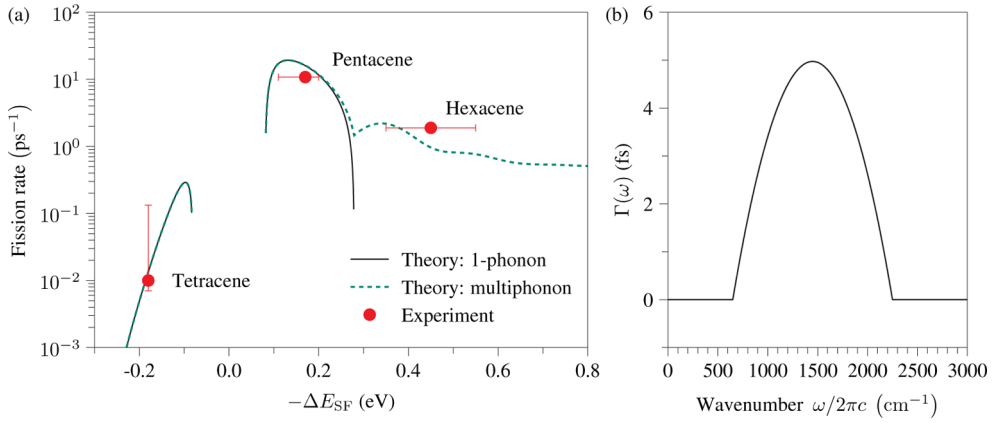

Figure 3. (a) Comparison of theoretical and experimental singlet fission rates. Red circles denote the experimentally measured singlet fission rates for tetracene, pentacene, and hexacene (left to right) with approximate error bars highlighting the spread of reported values (see text for references). Experimental rates are compared to the 1-phonon and multiphonon rate theories, for which only the latter is capable of capturing the SF rate of hexacene. (b) The spectral density employed in the calculations, which is representative of the high-frequency C=C stretching modes in acenes.

spectral signatures, the data are analyzed within the framework of global target analysis[31,32] (for details, see Supporting Information). This was performed for the full set of data, which includes absorption in the near IR and delay times up to 3000 ps. The data are well reproduced with a three-state model of SF depicted in the inset of Figure 2c, bottom: excitation from the ground state creates a singlet exciton, the singlet then undergoes SF to form triplets, and on a longer time scale the triplets decay to repopulate the ground state (triplet decay dynamics are included in the Supporting Information). This model intentionally neglects the fast (~ 100 fs), wavelength-dependent dynamics that can be observed near the high energy tail of the singlet absorption feature, since it (i) is uncorrelated to the rise of the triplet absorption feature, (ii) does not result in ground state repopulation, and (iii) is obscured at some wavelengths by coherent artifacts. While they do not influence the following analysis or conclusions, they are interesting to point out and may result from relaxation of the photoexcited or multiexciton transition state. The resultant model provides good kinetic fits and completely deconvolves the singlet and triplet into their respective time-independent, photoinduced absorption spectra (Figure 2b) and time-dependent population trajectories. In Figure 2c, we show the experimental kinetic traces and their fits (top) as well as the extracted population kinetics (bottom). This analysis yields a SF time scale of $k_{SF}^{-1} \approx$ 530 fs.

We note that singlet exciton deactivation via competing photoluminescence or intersystem crossing is safely neglected in our analysis. Like in solid-state pentacene, these processes are essentially unobserved in crystalline hexacene due to the rapid SF.[1,16,17] Similarly, as described above, we work at sufficiently low excitation density, ~ 6.3×10^{18} cm^{-3}, to neglect singlet−singlet annihilation,[20,33] especially in light of the fast (subpicosecond) SF rate. We conclude that effectively all singlet excitons undergo SF, resulting in a triplet quantum yield of nearly 200%. However, the SF time scale for hexacene (530 fs) is significantly slower than that for pentacene, despite the increased CT character discussed above.

In order to rationalize the decreased rate of SF in hexacene and to more broadly place hexacene within the family of acenes we have extended the theory developed in refs 6 and 7 to systems with a large exothermicity (for full details, see Supporting Information). To understand the required extension, note that if one only considers linear exciton−phonon coupling (characterized by a weighted phonon density of states, $\Gamma(\omega)$) treated at lowest order in perturbation theory, then the SF rate is given by[7]

$$k_{SF}(\Delta E_{SF} < 0, T) = \frac{8\pi V_{SF}^2}{\hbar}\frac{\lambda\omega_{ph}}{\Delta E_{SF}^2}\Gamma\left(-\frac{\Delta E_{SF}}{\hbar}\right)[N(-\Delta E_{SF}) + 1] \quad (1a)$$

$$k_{SF}(\Delta E_{SF} > 0, T) = \frac{8\pi V_{SF}^2}{\hbar}\frac{\lambda\omega_{ph}}{\Delta E_{SF}^2}\Gamma\left(\frac{\Delta E_{SF}}{\hbar}\right)N(\Delta E_{SF}) \quad (1b)$$

where λ is the vibrational reorganization energy, ω_{ph} is a characteristic phonon frequency, and $N(E) = [\exp(E/k_BT) - 1]^{-1}$ is the phonon thermal occupancy. Because $\Gamma(\omega)$ peaks at a characteristic vibrational frequency (roughly 1450 cm^{-1} for C=C stretching) and completely vanishes beyond a maximum frequency (roughly 3000 cm^{-1} for C−H stretching), the above expression predicts a rate which goes to zero for sufficiently large exothermicity, such as found in hexacene ($-\Delta E_{SF} \approx$ 500 meV ≈ 4000 cm^{-1}). This phenomenon is sometimes referred to as a phonon bottleneck and to capture the nonzero rate of SF in hexacene requires the inclusion of (slower) multiphonon relaxation effects.[34] Assuming that nonlinear exciton−phonon coupling terms treated to lowest order are dominant over linear coupling terms treated to higher order,[35] we can derive a rate law (see Supporting Information) which captures multiphonon processes:

$$k_{SF}(\Delta E_{SF} < 0, T) = \sum_{n=1}^{\infty} k_{SF}^{(n)}(-\Delta E_{SF}, 0)[N(-\Delta E_{SF}/n) + 1]^n \quad (2a)$$

$$k_{SF}(\Delta E_{SF} > 0, T) = \sum_{n=1}^{\infty} k_{SF}^{(n)}(\Delta E_{SF}, 0)[N(\Delta E_{SF}/n)]^n \quad (2b)$$

where

$$k_{SF}^{(n)}(\Delta E_{SF}, 0) = \frac{8\pi V_{SF}^2}{\hbar}\frac{\lambda\omega_{ph}}{\Delta E_{SF}^2}n!\alpha^{2n-2} \times\frac{1}{2\pi}\int_{-\infty}^{\infty} e^{i\Delta E_{SF}t/\hbar}\left(\int_0^{\infty}\Gamma(\omega)e^{-i\omega t}d\omega\right)^n dt \quad (3)$$

dx.doi.org/10.1021/ja503980c | J. Am. Chem. Soc. 2014, 136, 10654−10660

In the above expressions, n is the number of phonons emitted (or absorbed) and a new parameter α quantifies the importance of nonlinear exciton−phonon coupling terms ($\alpha = 0$ recovers the lowest-order expression, eq 1).

Employing the physically motivated model parameters V_{SF} = 30 meV, λ = 250 meV, and α = 0.55, we can accurately reproduce the SF rate behavior seen experimentally in tetracene, pentacene, and hexacene, as shown in Figure 3a. These results were obtained using a spectral density relevant for high-frequency optical phonons:

$$\Gamma(\omega) = \begin{cases} \frac{3}{4\Delta^3}[\Delta^2 - (\omega - \omega_{ph})^2], & \omega_{ph} - \Delta < \omega < \omega_{ph} + \Delta \\ 0, & \omega < \omega_{ph} - \Delta,\ \omega > \omega_{ph} + \Delta \end{cases} \quad (4)$$

with $\omega_{ph}/2\pi c$ = 1450 cm^{-1} and $\Delta/2\pi c$ = 800 cm^{-1}, characteristic of the acenes which are dominated by intramolecular C=C stretching modes.[36] This spectral density is plotted in Figure 1b. Low-frequency phonons are irrelevant due to their weak coupling to electronic transitions and small energy scales (∼10 meV) incapable of providing or accepting comparatively large energy differences (≳100 meV). For demonstrative purposes, we have assumed that the electronic coupling V_{SF} is the same for all materials, such that the observed behavior is entirely due to changes in the exothermicity ΔE_{SF}. The electronic coupling is only expected to vary by a factor of 2 or so over the range considered and for sufficiently large electronic couplings, the rate is expected to undergo a nonadiabatic to adiabatic transition, becoming independent of the coupling V_{SF}.[7,10]

We emphasize that our measured SF rate in hexacene places a much stricter requirement on competing theories than was previously available. In particular, viable kinetic theories for SF in acenes must explain the observed turnover in rate versus exothermicity. Extrapolating, we can make a prediction that crystalline heptacene should exhibit a still-smaller rate constant, with a time scale of of $k_{SF}^{-1} \approx 1-10$ ps. Our experimental and theoretical findings tighten the frequently quoted design criterion $\Delta E_{SF} < 0$. For the largest SF rates, one should strive for $-\Delta E_{SF} \approx E_{ph}$, where E_{ph} is an energy scale associated with the phonon degrees of freedom; crystalline pentacene almost perfectly satisfies this criterion, in accord with its ultrafast SF behavior.

A previously studied substituted hexacene derivative[25] provides an interesting, independent test of our theory. The solid-state hexacene derivative has a large exothermicity, $-\Delta E_{SF}$ = 650 meV,[25] and can be expected to have vibrational properties very similar to the unsubstituted acenes allowing a direct application of the present multiphonon theory. For this material, we can see from Figure 3a that the theory predicts a SF time scale of about 2 ps, which compares favorably to the experimentally measured time scale of 5.1 ps.[25] The remaining discrepancy can be attributed to the decreased electronic coupling due to poor packing, i.e., a smaller V_{SF} than used in Figure 3a.

A simplification of the above microscopic expression gives rise to an approximate "energy gap law" for the downhill, exothermic process, $k_{SF} \propto (V_{SF}/\Delta E_{SF})^2 \exp(\Delta E_{SF}/E_0)$, which is common in electron and energy transfer. This type of energy gap law qualitatively captures the rate reduction with increasing driving force and may be useful for simple interpretations of experimental data. However, we emphasize that an energy gap law is typically phenomenological and the microscopic rate expression presented here should be preferred. It is worth mentioning that there are other microscopic routes to multiphonon behavior and energy gap laws, including higher-order perturbation theory in the linear exciton−phonon coupling.[35] Such a protocol is responsible for the Englman-Jortner theories of radiationless transitions,[37] of which the low-temperature strong coupling limit was employed in Singh's early theory of SF.[38] Despite the apparent similarity with respect to turnover behavior, one should be cautious applying semiclassical Marcus-like theories which are only accurate for low-frequency phonons or at high temperatures, i.e., $\hbar\omega_{ph}/k_BT \ll 1$, which does not seem to be the case for the crystalline acene materials. For example, the latter will predict an unphysically strong temperature dependence even for exothermic SF. A proper quantum mechanical treatment of high-frequency phonons, as embodied in the present theory, predicts essentially no temperature dependence for the exothermic case of pentacene, in agreement with experiment.[11] Our theory does predict a slight temperature dependence for hexacene, providing an interesting−if not challenging−test of the multiphonon behavior proposed here. Specifically, the SF rate in hexacene is predicted to be temperature independent from 0 to 300 K, but to increase by roughly 15% at temperatures approaching 600 K (the melting/sublimation temperature of most acenes). The theory described here also predicts an activated, temperature dependence to the SF of tetracene. While early experiments found evidence of such activated behavior,[39,40] all recent experiments show temperature-independent SF,[20−22,41] suggesting that earlier measurements should be reinterpreted. We consider this to be an important topic for future study.

CONCLUSION

To summarize, we have elucidated important mechanistic features of SF by studying the electronic structure and ultrafast dynamics in crystalline hexacene. Combined with the wealth of existing results on tetracene and pentacene, our findings enable for the first time a systematic examination of trends in this prototypical family of molecules. More specifically, we have addressed (i) the dominant relaxation mechanism in hexacene crystals, i.e., ($S_1 \rightarrow 2 \times T_1$ + phonons) versus ($S_1 \rightarrow 3 \times T_1$); and (ii) the rate of SF in hexacene crystals and its interpretation within a unified theoretical framework. Regarding the first point, optical spectroscopy on polycrystalline and single crystals of hexacene has been combined with simple quantum chemistry arguments to conclude that ($S_1 \rightarrow 2 \times T_1$ + phonons) is the dominant relaxation pathway. In the context of photovoltaics, this implies that hexacene is suboptimal due to the excess energy wasted as heat. For the second point, we have performed ultrafast TA measurements on polycrystalline films to show that SF in hexacene is highly efficient but is significantly slower than in pentacene. We explain this turnover to a slower rate in hexacene by extending our previously developed theoretical model[6,7] to include multiphonon relaxation processes. Through this analysis, we conclude that SF to generate two triplets in hexacene imposes an exothermic driving force which is much larger than the energy of the available phonons. In turn, the SF process necessitates multiphonon relaxation processes that slow down the SF rate in comparison to pentacene. Interestingly, this conclusion implies that for longer acenes such as heptacene, the even-larger exothermicity combined with further increased CT

character may result in favorable conditions for the ($S_1 \rightarrow 3 \times T_1$) process.

EXPERIMENTAL SECTION

Sample Preparation and Characterization. Hexacene synthesis and single crystal growth were as reported in ref 19. Polycrystalline films were grown by a vapor-phase transport method. A source of hexacene (ca. 1 mg) was placed in the sublimation zone at 200 °C under vacuum (ca. 450 mTorr) with flowing high-purity argon (99.999%) as a carrier gas with a flow rate of 50 sccm. Fused silica substrate, which was coated with a self-assembled monolayer of octyltrichlorosilane was placed in the crystallization zone. Following preparation, both single crystals and polycrystalline films were transferred into a controlled-environment glovebox. Single crystal characterization involved examination under an optical microscope. Polycrystalline characterization involved grazing incidence wide-angle X-ray scattering measurements and scanning electron microscope imaging.

Reflectance Contrast Measurements. Broadband radiation from a tungsten quartz halogen source was focused on the sample by a 40× objective, yielding a spot of about 2 μm in diameter. The reflected signal was collected and analyzed with a grating spectrometer and a liquid nitrogen-cooled CCD with a spectral resolution of about 5 nm. Polarization angle-dependent measurements were performed by using a linear polarization filter. The reflectance was obtained by normalizing the sample signal to that of the bare fused silica substrate for each setting of the polarization angle.

Time-Resolved Spectroscopy. Ultrafast transient absorption experiments were conducted using a commercial Ti:sapphire laser (800 nm, 100 fs, 3.5 mJ @ 1 kHz). The experiment was conducted using a typical transmission pump−probe geometry utilizing the output of an optical parametric amplifier as the excitation source. Supercontinuum resultant from focusing fundamental on a sapphire disk was used as the probe source. Pump−probe delay is controlled using a translational stage to delay the probe pulse. The probe was split into signal and reference beams and detected on a shot-by-shot basis with dual fiber-coupled Si (visible) or InGaAs (infrared) photodiode arrays. All presented data were collected under anaerobic conditions with a substrate-probe angle of 45°.

ASSOCIATED CONTENT

Supporting Information

Synthesis, sample preparation and characterization, transient absorption, and theoretical formalism details. This material is available free of charge via the Internet at http://pubs.acs.org.

AUTHOR INFORMATION

Corresponding Author

oy2118@columbia.edu

Author Contributions

[‖]These authors contributed equally.

Notes

The authors declare no competing financial interest.

ACKNOWLEDGMENTS

Overall project coordination, sample growth and optical characterization were supported as part of the Center for Re-Defining Photovoltaic Efficiency Through Molecular-Scale Control, an Energy Frontier Research Center funded by the US Department of Energy (DOE), Office of Science, Office of Basic Energy Sciences under Award DE-SC0001085. O.Y. and E.B. were supported by the EFRC as a research fellows. We wish to thank Mikas Vengris (Vilnius University) for graciously providing his global analysis software package for our use. T.C.B. was partially supported by the Department of Energy Office of Science Graduate Fellowship Program (DOE SCGF), administered by ORISE-ORAU under contract no. DE-AC05-06OR23100. A.C. gratefully acknowledges funding from the Alexander von Humboldt Foundation within the Feodor-Lynen Fellowship program. Research was carried out in part at the Center for Functional Nanomaterials, Brookhaven National Laboratory, which is supported by the U.S. Department of Energy, Office of Basic Energy Sciences, under contract no. DE-AC02-98CH10886.

REFERENCES

(1) Smith, M. B.; Michl, J. *Chem. Rev.* **2010**, *110*, 6891.
(2) Smith, M. B.; Michl, J. *Annu. Rev. Phys. Chem.* **2013**, *64*, 361.
(3) Congreve, D. N.; Lee, J.; Thompson, N. J.; Hontz, E.; Yost, S. R.; Reusswig, P. D.; Bahlke, M. E.; Reineke, S.; Van Voorhis, T.; Baldo, M. A. *Science* **2013**, *340*, 334−337.
(4) Ehrler, B.; Walker, B. J.; Böhm, M. L.; Wilson, M. W.; Vaynzof, Y.; Friend, R. H.; Greenham, N. C. *Nature Comm.* **2012**, *3*, 1019.
(5) Havenith, R. W. A.; de Grier, H. D.; Broer, R. *Mol. Phys.* **2012**, *110*, 2445.
(6) Berkelbach, T. C.; Hybertsen, M. S.; Reichman, D. R. *J. Chem. Phys.* **2013**, *138*, 114102.
(7) Berkelbach, T. C.; Hybertsen, M. S.; Reichman, D. R. *J. Chem. Phys.* **2013**, *138*, 114103.
(8) Chan, W.-L.; Berkelbach, T. C.; Provorse, M. R.; Monahan, N. R.; Tritsch, J. R.; Hybertsen, M. S.; Reichman, D. R.; Gao, J.; Zhu, X.-Y. *Acc. Chem. Res.* **2013**, *46*, 1321.
(9) Beljonne, D.; Yamagata, H.; Brédas, J. L.; Spano, F. C.; Olivier, Y. *Phys. Rev. Lett.* **2013**, *110*, 226402.
(10) Yost, S. R.; Lee, J.; Wilson, M. W. B.; Wu, T.; McMahon, D. P.; Parkhurst, R. R.; Thompson, N. J.; Congreve, D. N.; Rao, A.; Johnson, K.; Sfeir, M. Y.; Bawendi, M.; Swager, T. M.; Friend, R. H.; A, M.; van Voorhis, T. *Nat. Chem.* **2014**, *6*, 492.
(11) Chan, W.-L.; Ligges, M.; Jailaubekov, A.; Kaake, L.; Miaja-Avila, L.; Zhu, X.-Y. *Science* **2011**, *334*, 1541.
(12) Casanova, D. *J. Chem. Theory Comput.* **2014**, *10*, 324.
(13) Yamagata, H.; Norton, J.; Hontz, E.; Olivier, Y.; Beljonne, D.; Brédas, J. L.; Silbey, R. J.; Spano, F. C. *J. Chem. Phys.* **2011**, *134*, 204703.
(14) Cudazzo, P.; Gatti, M.; Rubio, A. *Phys. Rev. B* **2013**, *86*, 195307.
(15) Berkelbach, T. C.; Hybertsen, M. S.; Reichman, D. R. Microscopic theory of singlet exciton fission. III. Crystalline pentacene, **2014**, submitted.
(16) Jundt, C.; Klein, G.; Sipp, B.; Le Moigne, J.; Joucla, M.; Villaeys, A. A. *Chem. Phys. Lett.* **1995**, *241*, 84.
(17) Wilson, M. W. B.; Rao, A.; Clark, J.; Kumar, R. S. S.; Brida, D.; Cerullo, G.; Friend, R. H. *J. Am. Chem. Soc.* **2011**, *133*, 11830.
(18) Wilson, M. W. B.; Rao, A.; Ehrler, B.; Friend, R. H. *Acc. Chem. Res.* **2013**, *46*, 1330.
(19) Watanabe, M.; Chang, Y. J.; Liu, S.-W.; Chao, T.-H.; Goto, K.; Islam, M. M.; Yuan, C.-H.; Tao, Y.-T.; Shinmyozu, T.; Chow, T. J. *Nat. Chem.* **2012**, *4*, 574.
(20) Burdett, J. J.; Gosztola, D.; Bardeen, C. J. *J. Chem. Phys.* **2011**, *135*, 214508.
(21) Chan, W.-L.; Ligges, M.; Zhu, X.-Y. *Nat. Chem.* **2012**, *4*, 840.
(22) Wilson, M. W. B.; Rao, A.; Johnson, K.; Gélinas, S.; di Pietro, R.; Clark, J.; Friend, R. H. *J. Am. Chem. Soc.* **2013**, *135*, 16680.
(23) Angliker, H.; Rommel, E.; Wirz, J. *Chem. Phys. Lett.* **1982**, *87*, 208−212.
(24) Roth, F.; Mahns, B.; Hampel, S.; amd H. Berger, M. N.; Büchner, B.; Knupfer, M. *Eur. Phys. J. B* **2013**, *86*, 66.
(25) Lee, J.; Bruzek, M. J.; Thompson, N. J.; Sfeir, M. Y.; Anthony, J. E.; Baldo, M. A. *Adv. Mater.* **2013**, *25*, 1445.
(26) Burdett, J. J.; Bardeen, C. J. *Acc. Chem. Res.* **2013**, *46*, 1312.
(27) Marciniak, H.; Pugliesi, I.; Nickel, B.; Lochbrunner, S. *Phys. Rev. B* **2009**, *79*, 235318.
(28) Hellner, C.; Lindqvist, L.; Roberge, P. C. *J. Chem. Soc., Faraday Trans. 2* **1972**, *68*, 1928.

(29) Bree, A.; Lyons, L. E. *J. Chem. Soc.* **1960**, 5206.
(30) Faltermeier, D.; Gompf, B.; Dressel, M.; Tripathi, A. K.; Pflaum, J. *Phys. Rev. B* **2006**, *74*, 125416.
(31) van Stokkum, I. H. M.; Larsen, D. S.; van Grondelle, R. *Biochim. Biophys. Acta* **2004**, *1657*, 82.
(32) Mullen, K. M.; Vengris, M.; van Stokkum, I. H. M. *J. Glob. Optim.* **2007**, *38*, 201.
(33) Fleming, G. R.; Millar, D. P.; Morris, G. C.; Morris, J. M.; Robinson, G. W. *Aust. J. Chem.* **1977**, *30*, 2353.
(34) Schaller, R. D.; Pietryga, J. M.; Goupalov, S. V.; Petruska, M. A.; Ivanov, S. A.; Klimov, V. I. *Phys. Rev. Lett.* **2005**, *95*, 196401.
(35) Egorov, S. A.; Skinner, J. L. *J. Chem. Phys.* **1995**, *103*, 1533.
(36) Girlando, A.; Grisanti, L.; Masino, M.; Brillante, A.; Della Valle, R. G.; Venuti, E. *J. Chem. Phys.* **2011**, *135*, 084701.
(37) Englman, R.; Jortner, J. *Mol. Phys.* **1970**, *18*, 145.
(38) Singh, J. *J. Phys. Chem. Solids* **1978**, *39*, 1207.
(39) Thørsmolle, V. K.; Averitt, R. D.; Demsar, J.; Smith, D. L.; Tretiak, S.; Martin, R. L.; Chi, X.; Crone, B. K.; Ramirez, A. P.; Taylor, A. J. *Phys. Rev. Lett.* **2009**, *102*, 017401.
(40) Burdett, J. J.; Bardeen, C. J. *J. Am. Chem. Soc.* **2012**, *134*, 8597.
(41) Tayebjee, M. J. Y.; Clady, R. G. C. R.; Schmidt, T. W. *Phys. Chem. Chem. Phys.* **2013**, *15*, 14797.